High Dielectric Constant Microwave Probes for Sensing Soil Moisture

J. ROBERT BIRCHAK, MEMBER, IEEE, C. GERALD GARDNER, MEMBER, IEEE, JACKIE E. HIPP, MEMBER, IEEE, AND JOE M. VICTOR, MEMBER, IEEE

Abstract—Implantable soil moisture sensors suitable for long-term monitoring of moisture in highway subgrades and for similar applications are needed. Two candidate designs of microwave sensors (operating range 4 to 6 GHz) have been investigated for such applications. One design uses the fringing field of a low-loss dielectric slab waveguide (relative dielectric constant of 25) to obtain good resolution for finely divided soil such as bentonite clay with moisture ranging from 10 to 50 percent by dry weight for effective sample volumes of 20 to 40 cm³. The response of the dielectric waveguide sensor has been calculated in terms of the effective dielectric constant of the soil–water mixture. A model based on index of refraction yields an effective dielectric constant in reasonable agreement with experiment when effects of ionic conduction are accounted for. Another sensor design, better adapted for coarse materials, such as crushed limestone aggregate, uses waves launched from a tapered dielectric slab. By using either frequency or spatial averaging methods, the launched wave sensor accommodated aggregate particles passed by a 0.63-cm mesh sieve, and was found to have satisfactory resolution for the range of 0- to 10-percent moisture by dry weight.

I. Introduction

THE DIPOLAR relaxation of water molecules results in an absorption of microwave energy which can be used to measure soil moisture [1]–[4]. The objective of this investigation is to interpret signals from microwave moisture sensors in terms of moisture-related variations in the effective dielectric constant of a soil–moisture mixture. Although microwave moisture densing is common practice [5]–[12], inexpensive sensors are needed that can be permanently implanted in soils and do not require measurement of the soil specimen's dimensions or confinement of the soil in a container. The implanted sensors must also be adaptable for a wide range of moisture levels and, in particular, must have good resolution at higher moisture levels where available microwave moisture sensors are relatively insensitive [7]–[13]. Additionally, the effective soil sample should be large enough to average over a volume large compared to soil particle size.

First, the calculation and measurement of the soil's effective complex dielectric constant ϵ^* are presented (as discussed in Appendix A, $\epsilon^* = \epsilon' - j\epsilon''$). Then, two experimental sensor designs are described, each of which operates in the 4- to 6-GHz range and incorporates low-loss high dielectric constant material (Stycast HiK®, $\epsilon' = 25$). One of the sensors, intended for use with finer grained soil at high moisture levels, employed a dielectric slab waveguide. The other, for low moisture levels and larger particle size, used tapered-dielectric transmitting and receiving antennas.

Manuscript received May 8, 1973; revised August 20, 1973. This work was supported in part by the Highway Research Board through the National Cooperative Highway Research Program under Project 21-2.

The authors are with Southwest Research Institute, San Antonio, Tex. 78284.

® Registered Trademark, Emerson and Cuming, Inc.

II. Calculation and Measurement of the Effective Dielectric Constant of Moist Soil

The dielectric constant of a mixture is not a unique function of the fractional volumes of the constituents but depends also on the geometric distribution. Brown [14] has demonstrated, for example, that in a layered structure formed of parallel plates with two alternating dielectric constants, the effective composite dielectric constant depends on orientation, being smaller when the electric field is perpendicular to the layers than when parallel. For an electric field parallel to the plate interfaces, Brown's model gives

$$\epsilon_m^* = f_1\epsilon_1^* + (1 - f_1)\epsilon_2^* \tag{1}$$

where ϵ_m^*, ϵ_1^*, and ϵ_2^* are the complex dielectric constants of the mixture, and the two constituents, respectively; and f_1 is the fractional volume of the first constituent (f_1 = volume of first constituent/total volume). Equation (1) is equivalent to the volume-averaged dielectric constant and will be referred to as the "volumetric mixing model." The model ignores the filling of voids, hydration, and ionic effects. As will be shown, (1) is not in good agreement with our experimental results.

Brown [14] further describes several other models for other mixing geometries. He shows, for example, that when the electric field is perpendicular to alternating layers, the reciprocal of ϵ_m^* equals the sum of the reciprocals of ϵ_1^* and ϵ_2^* multiplied by their respective fractional volumes. He also discusses the Clausius–Mossotti model [14] which treats dilute solution of one species of polar molecules in another. The latter two models were also found to be unsatisfactory for describing our experimental results, perhaps because both models assume geometric shapes which give large depolarization fields in the water [15].

For improved agreement with experiment, we propose a model based on the optical path length of a single electromagnetic ray. As shown in Appendix B, the complex dielectric constant of the soil–water mixture ϵ_m^* is given by

$$\sqrt{\epsilon_m^*} = f_1\sqrt{\epsilon_1^*} + (1 - f_1)\sqrt{\epsilon_2^*} \tag{2}$$

where the subscripts 1 and 2, respectively, designate water and dry soil. (Experimentally, f_1 was the ratio of the volume concentration of water to the density of pure water.) Equation (2) is equivalent to a volumetric average of the complex index of refraction, and will be referred to as the index of refraction mixing model. Equation (2) is almost equivalent to Paquet's empirical expression for the moisture of mortar [12]. The value of ϵ_m^* calculated from (2) is smaller than that from (1), but not as small as that from the alternating plates with perpendicular electric field model, or the Clausius–Mossotti model.

TABLE I
MEASURED AND CALCULATED COMPLEX DIELECTRIC CONSTANT $\epsilon^* = \epsilon' - j\epsilon''$ FOR BENTONITE CLAY MIXED WITH WATER (4 GHz)
(f_1 is the fractional volume of water)

	Measured			Volumetric Mixing Model		Index of Refraction Model	
f_1	ϵ'	ϵ''	$\epsilon'' - \sigma_i/\omega\epsilon_0$	ϵ'	ϵ''	ϵ'	ϵ''
0.0085	2.5	0.11	0.1				
0.00				1.9	0.03	2.3	0.08
0.063	3.8	0.93	0.63	6.5	1.3	3.8	0.37
0.19	7.8	2.6	1.1	16	3.7	8.4	1.4
0.28	12	5.2	2.5	23	5.5	13	2.4

Equations (1) and (2) can be compared with our measurements. Table I compares calculated dielectric constants with values experimentally measured on Wyoming bentonite clay. The experimental procedure used to measure ϵ^* is described in Appendix A. The dielectric constant ϵ_2^* for dry soil ($f_1 = 0.0$) was estimated by extrapolating from the lowest attainable level, $f_1 = 0.0085$ (determined by the gravimetric method). By comparing experimental and calculated results one finds that (2) estimates ϵ' fairly well. The rather large values of ϵ'' observed at 4 GHz result partially from ionic conduction. When $\sigma_i/\omega\epsilon_0$ (see Appendix A) is subtracted from ϵ'' to compensate for ionic conduction, the remaining (nonionic) part of ϵ'' agrees rather well with the value of ϵ'' calculated from (2).

III. SENSOR FOR HIGH MOISTURE LEVELS IN FINE-GRAINED SOILS

A special sensor was designed for monitoring very moist fine-grained soils ($f_1 > 0.2$). For high moisture levels the small penetration depth of microwaves makes it difficult to obtain adequate effective sample size. When a TEM wave encounters (at normal incidence) a plane interface between air and very moist soil, the wave penetrates a depth δ given by [15],

$$\delta \simeq \lambda_0 \sqrt{\epsilon'}/\pi\epsilon'' \qquad (\text{for } \epsilon'' \ll \epsilon') \tag{3}$$

(λ_0 is the free space wavelength). Because the penetration depth decreases when ϵ'' increases, most microwave moisture sensors have decreasing resolution with increasing moisture [7], [13]. To obtain optimum resolution at high moistures, a dielectric slab waveguide sensor design was investigated. The sensor (shown schematically in Fig. 1) has a TM wave inserted from the conductive coupling cavity into a low-loss dielectric slab. The wave propagates along the slab to a diode detector. When the dielectric constant of the slab is much greater than that of the moist soil, very little energy fringes into the soil and the intensity reaching the detector is only slightly attenuated. When, however, with rising moisture content the soil's effective dielectric constant approaches that of the slab, more and more of the energy fringes into the comparatively lossy soil, and the intensity attenuates rapidly. A schematic diagram of the experimental arrangement used is shown in Fig. 2.

The fields and attenuation in the slab and the moist soil can be calculated, provided simplifying assumptions are made. The following calculations consider only the lowest order propagation mode and assume infinite extent in the y direction (dielectric slab width large compared to slab thickness) [16]. The y direction is taken to be parallel to the soil–dielectric interface, and perpendicular to the z axis, which is taken to be the direction of propagation (see Fig. 1). At the

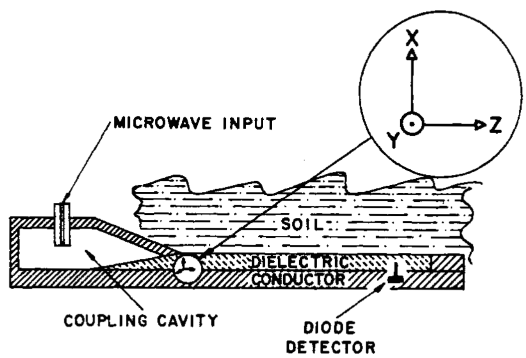

Fig. 1. Schematic diagram of dielectric waveguide microwave moisture sensor. Soil–dielectric interface 3.7 cm wide, 10 cm long; slab thickness 0.63 cm; Schottky barrier diode with quarter wavelength antenna; 4–7 GHz; dielectric constant 25.

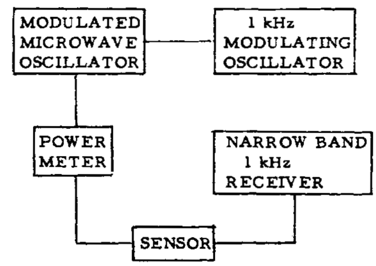

Fig. 2. Block diagram of principal electronic components required for moisture sensor.

conductor–slab interface $x = 0$; at the slab–soil interface $x = b$; and at the start of the slab–soil interface $z = 0$.

Maxwell's equations for dielectric layers, solved elsewhere [15], have been used to obtain the y component of the magnetic field in the dielectric slab to be

$$H_d = H_0 e^{-\gamma_s z} \cos k_d x \tag{4}$$

and in the soil to be

$$H_m = H_0 e^{-\gamma_s z} e^{-k_m (x-b)} \cos k_d b \tag{5}$$

where H_0 is the magnetic field intensity at $x = z = 0$ and the constants γ_s, k_d, and k_m are complex numbers the values of which are determined by the boundary conditions. If the complex dielectric constants of (moist) soil and the dielectric slab are, respectively, designated by ϵ_m^* and ϵ_d^*, application of the boundary conditions results in three simultaneous equations [15]–[17]:

$$k_m^2 = \omega^2 \mu \epsilon_m^* - \gamma_s^2 \tag{6}$$

$$k_d^2 = \omega^2 \mu \epsilon_d^* - \gamma_s^2 \tag{7}$$

$$\frac{\epsilon_m^*}{\epsilon_d^*} = \left[\frac{\omega^2 \mu \epsilon_m^* - \gamma_s^2}{\omega^2 \mu \epsilon_d^* - \gamma_s^2}\right]^{1/2} \coth\left(jb\sqrt{\omega^2 \mu \epsilon_d^* - \gamma_s^2}\right) \tag{8}$$

where μ is the magnetic permeability.

In designing a dielectric slab type of moisture sensor, two parameters are of primary importance, i.e., the signal strength from the detector and the effective volume of soil sampled. The signal strength S from the square-law diode detector [18] is approximately

$$S = S_0 e^{-2\gamma_s z_d} \tag{9}$$

where S_0 is the signal strength at $z = 0$, and z_d is the propagation distance to the detector. The slab–soil system's complex

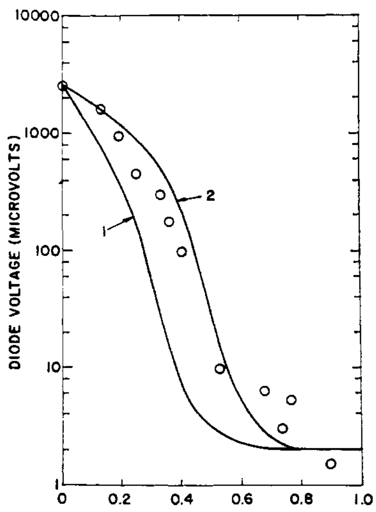

Fig. 3. Response of microwave sensor versus volume concentration of water in bentonite clay. Circles, experimental; curve 1 from dielectric mixing model; curve 2 from index of refraction mixing model; input power 1 mW (4.75 GHz modulated 1000 Hz).

propagation constant γ_s is $\gamma_s = \alpha_s + j\beta_s$ where α_s and β_s are the system's attenuation and phase constants, respectively. Since the detector was a quarter wavelength from the short-circuit termination of the slab, one finds from (9) that α_s must be estimated in order to predict signal strength.

Equation (8) can be solved for the complex γ_s to obtain α_s. Since (8) gives an attenuation which depends on the dielectric constant of moist soil, the calculated signal strength depends on the model chosen for estimating the dielectric constant of the water–soil mixtures. Fig. 3 presents graphically calculated and experimental results, showing that the measured signal strengths fall between two theoretical curves. Numerically solving (8) by Newton's method on a digital computer gave curves 1 and 2, corresponding to the dielectric mixing models expressed in (1) and (2), respectively. As expected from the results in Table I, (1) (the volumetric mixing model) yields too large a value for ϵ' with the consequence that curve 1 is shifted to the left. On the other hand, (2) is not corrected for ionic conduction and gives ϵ'' too small a value. The predicted signal value, therefore, does not decrease rapidly enough so that curve 2 lies slightly above the experimental values.

The effective volume of sampled soil depends on the penetration depth h of the fringing field, which is related [16] to the real part of k_m (i.e., $h = [\mathrm{Re}\ k_m]^{-1}$). For a frequency of 4.75 GHz and slab thickness b of 0.63 cm, the fringing field of our experimental sensor penetrated approximately 0.2 cm at low moistures and 1.0 cm for high moistures, which gave matched soil and slab dielectric constants. Since the active surface of the sensor dielectric slab was about 37 cm², the sampled volume was between 20 and 40 cm³ at high moisture levels.

IV. Sensor for Low Moisture Levels in Coarse-Grain Soils

For low moistures and large particle size, a second sensor was designed such that all dimensions of the sampled volume were large compared to particle size. As shown in Fig. 4, the sensor was designed to launch a wave from a transmitting tapered dielectric slab to a receiving dielectric wedge, housing a diode detector and antenna. The electronic components were otherwise the same as those in Fig. 2. This sensor configuration avoids the problem of confining a fixed thickness of soil between two antenna horns [7]. Since the wave radiates from the tapered slab, the signal strength at the detector depends primarily on the amount of attenuation due to water in the soil and becomes too small to be detected at high moisture levels ($f_1 > 0.2$). The broad radiation pattern irradiates a large effective sample volume, making the sensor suitable for large particle size (e.g., crushed limestone).

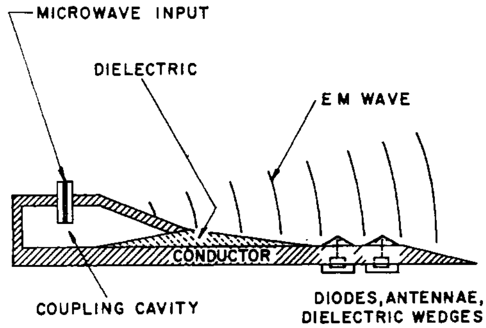

Fig. 4. Schematic diagram of launched-wave microwave moisture sensor. Tapered launcher 3.7 cm wide, 10 cm long, maximum thickness 0.63 cm; detectors at 14 and 17.5 cm from start of launcher–soil interface.

In using the launched wave technique, one must consider possible coherently interfering signals. Because large particles and other inhomogeneities scatter the electromagnetic waves, the signal at the detector depends not only on the dielectric absorption but also on the geometrical arrangement of the constituent particles. Some of the scattered waves reach the detector by traveling a different path length from those of the primary signal, causing wave interference. For a single secondary scattered wave, the net field at the detector is

$$H = H_0[e^{-\gamma z} + Fe^{-\gamma d}] \tag{10}$$

where z is the distance from the radiator to the detector, H_0 is the magnetic field intensity at $z=0$, d is the effective secondary distance which goes from radiator to inhomogeneity to detector, and F is a factor giving the relative strength of the scattered wave signal. The signal amplitude of the square-law detector is therefore

$$S = KHH^* = KH_0^2e^{-2\alpha z}[1 + 2Fe^{-\alpha(d-z)} \cdot \cos\beta(d-z) + F^2e^{-2\alpha(d-z)}] \tag{11}$$

where K is a fixed proportionality constant.

To reduce the dependence of the measured signal on the effects of interfering signals, two types of averaging were studied: frequency and spatial. The most satisfactory frequency averaging was found to be the geometric mean of responses for each of n different frequencies:

$$\bar{S}_f = [S_1 \times S_2 \times \cdots \times S_n]^{1/n} \simeq KH_0^2e^{-2\bar{\alpha}z}\left[1 + \frac{2F}{n}\sum_n e^{-\alpha_i(d-z)}\cos\beta_i(d-z)\right] \tag{12}$$

where $\bar{\alpha}$ is the arithmetic mean attenuation for the n frequencies involved (terms of order $F^2e^{-2\alpha(d-z)}$ or higher are neglected). Analogously, the geometric mean signal for m different spatial locations of the receiving diode is

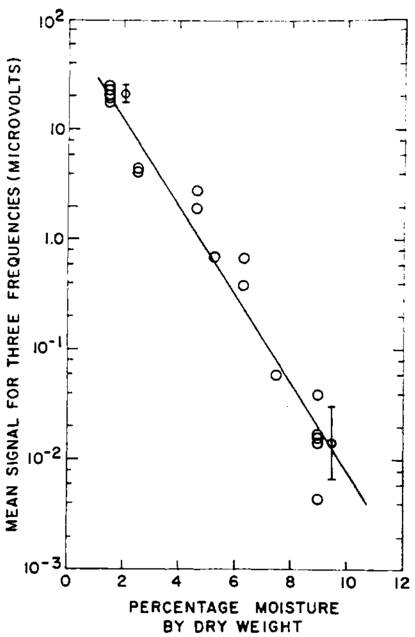

Fig. 5. Response of launched-wave sensor to moisture in coarse (0.63-cm mesh sieve) crushed limestone. Frequency-averaging method; 4.2, 4.75, and 5.8 GHz; results normalized to 1-mW input power. Error bars show standard deviations for 1.5- and 9-percent moisture.

$$\overline{S}_s = KH_0^2 e^{-2\alpha\bar{z}}\left[1+\frac{2F}{m}\sum_m e^{-\alpha(d_i-z_i)}\cos\beta(d_i-z_i)\right] \quad (13)$$

where $\bar{z}$ is the arithmetic mean radiator-to-detector distance. When α is small compared to β and $Fe^{-\alpha(d-z)}<1$, the terms multiplying F approach zero for large n and m, provided the arguments of the cosines have random values. Hence, for frequency and spatial averaging, (12) and (13) become identical with (9) except that the attenuation $\bar{\alpha}$ for frequency averaging is the average for all frequencies used and the distance $\bar{z}$ for spatial averaging is the mean radiator-to-detector distance.

Experimental results were obtained for only three frequencies and two spatial locations of detectors. The predicted exponential dependence of the averaged results is observed in Figs. 5 and 6. Fig. 6 shows the four bentonite clay observations as well as the crushed limestone data. Table II presents the standard errors of estimate for log S and the correlation coefficients from regression analysis. The averaged values had smaller standard error than most of the sets of unaveraged values. One unaveraged data set, however (obtained by a fortuitous choice of frequency and detector distance), had smaller error than the averaged data. In practice the optimum frequency and detector distance will depend on soil types, particle size, and packing, and it will be impractical to individually optimize sensors for each burial site. Averaging can therefore simplify design and installation. Statistical analysis using f_l instead of composition (percent moisture by dry weight) as the independent variable gave essentially the same errors when the crushed limestone data were analyzed. But when an attempt was made to fit both crushed limestone and bentonite clay to the same regression equation, f_l produced larger error than percent moisture by dry weight. This is to be expected because for small f_l, larger attenuation was observed for bentonite clay than for limestone, and the limestone was more dense than the clay.

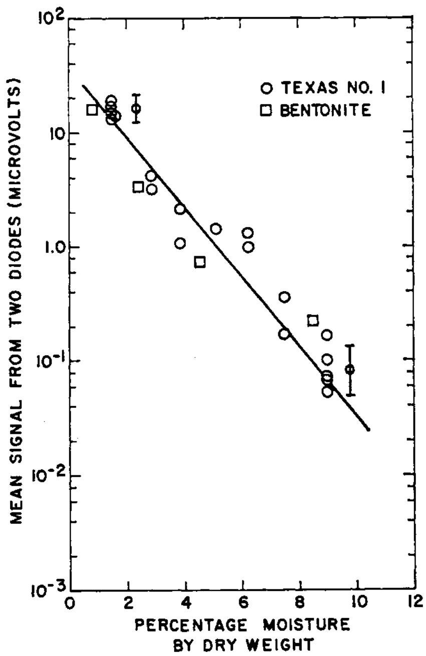

Fig. 6. Response of launched-wave sensor to moisture in coarse crushed limestone and in bentonite clay. Spatial averaging method; detectors at 14 and 17.5 cm; frequency 4.2 GHz. Error bars show standard deviations for 1.5- and 9-percent moisture.

TABLE II
REGRESSION CORRELATION COEFFICIENT R AND STANDARD ERROR (SE) OF SIGNAL LOGARITHM VERSUS MOISTURE (PERCENT DRY WEIGHT)

Method of Averaging	Crushed Limestone (19 observations)		Limestone (19 observations) Clay (4 observations)	
	R	SE	R	SE
Unaveraged	−0.92 to −0.99	0.46 to 0.16	−0.92 to −0.97	0.55 to 0.23
Frequency (4.2, 4.75, and 5.8 GHz)	−0.98	0.20	−0.94	0.30
Spatial (14 and 17.5 cm)	−0.97	0.31	−0.97	0.22

V. Conclusion

In principle, the results obtained show that a dual probe combining both the slab waveguide and the launched wave sensor could be used to monitor soil moistures over the range $0<f_l<0.5$. Good resolution can be obtained for even higher moistures if a higher dielectric constant slab is used. The specimen size, moreover, can be relatively large, e.g., greater than 30 cm^3. An implantable microwave sensor is, therefore, feasible.

The development of a practical fieldworthy sensor based on the approach we have investigated will require further investigations of sensor calibration, measurements in various materials, averaging of effects of reflections from inhomogeneities, and compensation for ionic conduction and for temperature dependence of the dielectric constant of moist soil. The results in Figs. 3, 5, and 6 do indicate that the probe response, for specific materials, can be empirically calibrated to yield moisture levels. The frequency and spatial averaging techniques, moreover, when adequately developed, should reduce the spurious effects of inhomogeneities within the effective volume of an implanted sensor.

Provided that ionic conductivity sensors and thermometers can be incorporated to permit compensation for variations in ionic conduction and temperature, the microwave sensors of the types investigated offer a promising method of monitoring subsurface soil moisture levels.

Appendix A

Discussion of the Complex Dielectric Constant and its Measurement

A medium's complex dielectric constant ϵ^* which has real component ϵ' and imaginary component $-\epsilon''$ can be determined by measurement of the medium's complex propagation constant γ.

The complex propagation constant of an unbounded homogeneous isotropic medium is commonly expressed as [15]

$$\gamma \triangleq \sqrt{j\omega\mu(\sigma + j\omega\epsilon)} \tag{14}$$

where μ, σ, and ϵ are the real permeability, conductivity, and permittivity of the medium. The permeabilities of the soils investigated in this program were approximately μ_0, the permeability of free space. The real conductivity and permittivity are related to the complex dielectric constant ϵ^* by

$$\epsilon^* \triangleq \frac{\epsilon}{\epsilon_0}\left(1 - j\frac{\sigma}{\omega\epsilon}\right) \tag{15}$$

where ϵ_0 is the permittivity of free space. Consequently, (14) may be condensed to

$$\gamma = j\omega\sqrt{\mu_0\epsilon_0}\sqrt{\epsilon^*}. \tag{16}$$

The complex propagation constant of a soil may be calculated from impedance measurements made on a section of uniform coaxial transmission line filled with the soil by the relation

$$\gamma = \frac{1}{l}\tanh^{-1}\sqrt{Z_{sc}/Z_{oc}} \tag{17}$$

where

- l length of coaxial transmission line;
- Z_{sc} input impedance of the soil-filled transmission line terminated by a short circuit;
- Z_{oc} input impedance of the soil-filled transmission line terminated by an open circuit.

Equations (14), (16), and (17) may be combined to express the complex dielectric constant of the soil as

$$\epsilon^* = -\frac{1}{\mu_0\epsilon_0}\left(\frac{1}{\omega l}\tanh^{-1}\sqrt{Z_{sc}/Z_{oc}}\right)^2. \tag{18}$$

The open- and short-circuit impedances were derived from measurements made with a precision slotted line [19]. The soil sample was packed uniformly at the desired density in a short section of rigid coaxial air line. Lower frequency measurements between 300 MHz and 4 GHz were made to resolve ambiguities in the inverse hyperbolic tangent function. (The ambiguities arise due to the uncertain number of half wavelengths within the soil-filled transmission line.)

In addition, the lower frequency measurements were useful for estimating the effects of ionic conductivity in the moist soils. Due to ionic conduction [3], [20] the dielectric constants measured at 300 MHz were larger than those at 4 GHz. The linear relation between ϵ^* and ω^{-1} observed at the lower frequencies indicated, however, that the effects of ionic conduction at 4 GHz can be subtracted.

The total complex dielectric constant ϵ_T^* of moist soil was assumed to be composed of ionic and nonionic contributions

$$\epsilon_T^* = \epsilon_m^* + \epsilon_i^* = \epsilon_m^* + \epsilon_i' - j\frac{\sigma_i}{\omega\epsilon_0} \tag{19}$$

where ϵ_m^*, the dielectric constant from (1) or (2), depends only on the complex dielectric constants of pure water and dry soil. The terms ϵ_i' and σ_i represent the contributions of ionic mobility to the real part of the dielectric constant and to the conductivity. Equation (19) can estimate σ_i by using the dielectric constants measured at low frequencies. Since the real part of ϵ_m^* is essentially constant below 1 GHz, the slope of the real part of ϵ_T^* gives ϵ_i'. Substituting the observed slope into (19) indicated that ϵ_i' contributed less than 15 percent to the measured value of ϵ' in Table I. Since the imaginary part of ϵ_m^* increased with frequency between 0.3 and 4 GHz and is quite small at 0.3 GHz, $\sigma_i/\omega\epsilon_0$ is closely approximated by the imaginary part of the dielectric constant measured at 0.3 GHz. Table I shows the results of subtracting the estimated $\sigma_i/\omega\epsilon_0$ from the observed ϵ'' at 4 GHz to compensate for ionic conduction.

Appendix B

Derivation of Effective Dielectric Constant for Fine-Grained Soils

Consider a plane electromagnetic wave propagating through an inhomogeneous medium, the attenuative effects of which are due solely to absorption, which can be accounted for through a complex propagation constant. For simplicity, assume that the propagation constant is a function of the z coordinate only. It is elementary to demonstrate that the amplitude of electric field intensity may be expressed in the form

$$E(z) = E_0 e^{-\int_0^z \gamma(z')dz'} = E_0 e^{-\bar{\gamma} z} \tag{20}$$

where $\bar{\gamma}$ is the effective average propagation constant,

$$\bar{\gamma} = \frac{1}{z}\int_0^z \gamma(z')dz'. \tag{21}$$

If the inhomogeneous mixture consists of a homogeneous matrix of one material in which particles of a second material are imbedded (the particle size being small compared to the wavelength of the electromagnetic wave), the effective propagation constant may be obtained by partitioning the integral in (21) into respective contributions from each of the two materials in question, giving the result

$$\bar{\gamma} = \gamma_1 l_1/z + \gamma_2 l_2/z \tag{22}$$

where the subscripts 1 and 2 refer, respectively, to the two materials, and $l_1 + l_2 = z$. By considering a unit area of the propagating plane wave, (22) may be expressed in the equivalent form

$$\bar{\gamma} = f_1\gamma_1 + f_2\gamma_2 \tag{23}$$

where f_1 and f_2 are the respective volumetric fractions of the two materials.

Assuming that the magnetic permeabilities of all constituents are equal to that of free space, (16) and (23) give

$$\sqrt{\epsilon_m^*} = f_1\sqrt{\epsilon_1^*} + f_2\sqrt{\epsilon_2^*} \tag{24}$$

which is equivalent to (2).

ACKNOWLEDGMENT

The dielectric constant of bentonite clay was measured using equipment developed for the United States Army Mobility Equipment Research and Development Center, Fort Belvoir, Va., under Contract DAAK02-72-C-0638.

REFERENCES

[1] P. Hoekstra and P. Cappillino, "An analysis of nondestructive sensing of water content by microwaves," Cold Regions Res. and Eng. Lab., Hanover, N. H., Res. Rep. 295, July 1971.
[2] J. R. Lundien, "Terrain analysis by electromagnetic means," U. S. Army Corps of Engineers, Vicksburg, Miss., Tech. Rep. 3-693, Sept. 1966.
[3] A. von Hippel, *Dielectric Material and Applications*. New York: Wiley, 1954.
[4] E. H. Grant, T. J. Buchannan, and H. F. Cook, "Dielectric behavior of water at microwave frequencies," *J. Chem. Phys.*, vol. 26, pp. 156–161, Jan. 1957.
[5] R. B. Bosisio, M. Giroux, and D. Couderc, "Paper sheet moisture measurements by microwave phase perturbation techniques," *J. Micr. Power, Canada*, vol. 5, pp. 25–34, Mar. 1970.
[6] R. J. Botsco, "Microwave moisture measurement," *Instrum. Cont. Syst.*, vol. 43, pp. 116–117, May 1970.
[7] ——, "Nondestructive testing of plastics with microwaves," *Plastics Des. Proces.*, vol. 8, pp. 1–9, Nov. 1968.
[8] S. Summerhill, "Microwaves in the measurement of moisture," *Instrum. Rev.*, vol. 14, pp. 419–422, Oct. 1967.
[9] H. B. Taylor, "Microwave moisture measurement," *Indust. Electron.*, vol. 3, pp. 66–70, Feb. 1965.
[10] W. A. G. Voss, "Microwave instruments for material control. I. A review," *J. Micr. Power, Canada*, vol. 4, pp. 210–216, Oct. 1969.
[11] M. Kent, "The use of strip-line configurations in microwave moisture measurement," *J. Micr. Power*, vol. 7, pp. 185–193, Mar. 1972.
[12] J. Paquet, "Mesure d'humidite in-situ par les methodes dielectriques, application au beton," *Mater. Construct.*, vol. 4, pp. 87–100, Mar. 1971.
[13] W. L. Curtis and R. J. Coe, "A microwave technique for the measurement of the dielectric properties of soils," *IEEE Trans. Microwave Theory Tech.*, vol. MTT-11, pp. 211–212, May 1963.
[14] W. F. Brown, "Dielectrics," in *Encyclopedia of Physics*, vol. 17. Berlin: Springer, 1956.
[15] W. Ramo, J. R. Whinnery, and T. Van Duzer, *Fields and Waves in Communications Electronics*. New York: Wiley, 1965.
[16] E. A. J. Marcatili, "Dielectric rectangular waveguide and directional coupler for integrated optics," *Bell Syst. Tech. J.*, vol. 48, pp. 2071–2102, Sept. 1969.
[17] J. E. Goell, "A circular-harmonic computer analysis of rectangular dielectric waveguides," *Bell Syst. Tech. J.*, vol. 48, pp. 2133–2159, Sept. 1969.
[18] A. F. Harvey, *Microwave Engineering*. New York: Academic Press, 1963, p. 759.
[19] J. E. Hipp, "Soil electromagnetic parameters as functions of frequency, soil density, and soil moisture," this issue, pp. 98–103.
[20] A. Stogryn, "Equations for calculating the dielectric constant of saline water," *IEEE Trans. Microwave Theory Tech.*, vol. MTT-19, pp. 733–736, Aug. 1971.

Soil Electromagnetic Parameters as Functions of Frequency, Soil Density, and Soil Moisture

JACKIE E. HIPP, MEMBER, IEEE

***Abstract*—Measurements are made to determine the conductivity and dielectric constants of a gray clay loam and a reddish-brown clay loam. The measurements are made as a function of soil density (from 1.2 g/cm³ to 1.8 g/cm³), soil moisture (from 0 percent to 20 percent of the dry soil weight), and excitation frequency (from 30 MHz to 4 GHz), using standard transmission line techniques. A correction term is presented to allow the effective open-circuit and short-circuit connections to be placed at any convenient location with respect to the soil–air interface.**

I. INTRODUCTION

THE conductivity and dielectric constants of two basic soil types have been determined as functions of frequency, moisture content, and density. The calculations were made from measurements of the propagation characteristics of a rigid coaxial transmission line filled with the soil. The measurements were made for frequencies from 30 MHz to 4 GHz, for moisture content from 0 percent to 20 percent (of dry soil weight), and for equivalent dry soil densities from 1.2 to 1.8 g/cm³.

Manuscript received May 8, 1973; revised August 20, 1973. This work was supported by the U. S. Army Mobility Equipment Research and Development Center, Fort Belvoir, Va., under Contract DAAK02-72-C-0018.
The author is with the Southwest Research Institute, San Antonio, Tex. 78284.

II. METHODS OF PARAMETER CALCULATION

A. Basic Theory of Electromagnetic Parameter Determination

The transverse electromagnetic (TEM) propagation characteristics of an unbounded, linear, isotropic, homogeneous material are identically the TEM propagation characteristics of a transmission line that has been homogeneously filled with a sample of that material. This is true, provided the mechanical parameters of the material (i.e., density, moisture, temperature, etc.) are not modified. If any one of the three constitutive parameters (permeability, permittivity, or conductivity) is known, the other two may be found directly from a knowledge of the TEM complex propagation constant. (The permeability of each of the soil types examined in this analysis is assumed to be that of free space.)

The relation between the characteristic impedance and the propagation characteristics of a lossy dielectric coaxial transmission line is found by solving Maxwell's equations